Analysis on Electromagnetic Heating and Spray Formation of Ethanol Fuel in Local-contact Microwave-heating Injector (LMI) System

LUKAS KANO MANGALLA*)
Mechanical Engineering Department
Halu Oleo University
Jl. HEA Mokodompit Kendari 93232
INDONESIA

HIROSHI ENOMOTO
Natural Science and Technology
Kanazawa University,
Kakuma –Machi Kanazawa Ishikawa, 9201192
JAPAN

USMAN RIANSE, YULIUS B. PASOLON
Agricultural Department
Halu Oleo University
J. HEA Mokodompit Kendari 93232
INDONESIA

*) E-mail: lk.mangalla@gmail.com

Abstract: - Heating fuel system becomes an important solution for utilizing bio-ethanol fuel in internal combustion engine to improve atomization and evaporation of the spray. A novel heating system of fuel flow inside the injector using electromagnetic heating is applied in LMI system. Comprehensive study on ethanol microwave heating and it is the effect on spray performances of the LMI system was conducted numerically and experimentally. Numerical modeling was developed in COMSOL Multiphysics to simulate the heating performances of ethanol inside the heating zone where the electromagnetic heating process occurred. The important phenomena of electromagnetism, heat transfer and fluid flow were solved based on the implicit method using Backward Differentiation Formula (BDF) solver. Electromagnetic heating performances were evaluated by comparing several parameters design such as geometry, size and shape of the heating zone. Spray characteristics of fuel injected were experimentally evaluated by measuring the droplets diameter and distribution. These properties were evaluated by using a laser dispersion spray analyzer (LDSA) and high speed camera. Spray formation can be evaluated from images captured during injection. Image analysis was conducted using Images-J to investigate the effect of electromagnetic heating on the breakup of the droplets. Simulation results indicate the dependency of fuel temperature distribution on the spatial and temporal distribution of electric field inside heating area. Fuel temperature was evaluated at the tip of the injector and both simulation and experimental results were found to satisfy the agreement. An increasing of fuel temperature tends to improve the atomization and provides the small droplet dispersion during electromagnetic heating.

Key-Words: LMI system, Heating performance, Microwave heating, Injector, Ethanol and Spray formation

1 Introduction

Regulation of exhaust gas emissions from internal combustion (IC) engine is recently very strict in many countries. Governments are using legislation to expedite transition towards a low emission vehicles such as (SULEV) in Japan and America since 2005, and Euro-5 in Europe countries. Therefore, the urgency for clean, efficient and affordable combustion strategies is becoming an important issue that must be addressed for automotive industries.

For the environmental and fuel resource assertions, bio-ethanol is a promising alternative fuel for gasoline. High oxygen content as well as octane number are the main advantages of this fuel that can improve combustion performances leading to a higher efficiency, knocking resistance and lower combustion emissions [1-2]. However, the utilization of ethanol in IC engine is limited by the

low calorific value and higher boiling point (Table 1). High ethanol blended in fuel may face the cold-start problem during combustion due to the lack of vaporization and boiling point [3-4]. Hence, the development of injection strategies is essential for employing ethanol in IC engine to improve fuel evaporation[5].

Many researchers proposed technical solution to improve fuel atomization and evaporation throughout the direct heating the fuel, using electric heating, inside injector and/or combustion chamber [7-9]. However, it was reported that some losses to another components of the engine can not be avoided. A new heating process of fuel flow inside injector is developed using microwave heating and this is called Local-contact Microwave-heating Injector or LMI [10-12]. Heating process of fuel flow occures inside heating zone, a small chamber created inside tip of injector. Electromagnetic wave power at frequency of 2.45GHz introduces into heating zone through the coaxial cable installed inside injector body (Fig 1 and Fig. 2). This heating process can heat-up the fuel much higher energy efficiency and more responsive than conventional heating since heat is generated due to the polarization of electromagnetic wave inside material [13]. Microwave forces the dipole molecule of water content in the material to rotate in high frequency to generate heat [13-14]. Initial investigation on performance spray and mechanical response of the LMI injector have been reported in ref [15]. The Injector system was developed to meet the demand on excellent spray formation, penetration and evaporation of fuel into combustion chamber [6, 16].

Advance numerical modeling is proposed to simulate the electromagnetic wave heating process occured in the heating zone of LMI injector. This study aims to analyze the electromagnetic heating characteristics of ethanol and to analyze the effect of microwave heating on the spray formation of the injected fuel.

Table 1. Properties of ethanol and gasoline

Property	Ethanol	Gasoline
Chemical formula	C_2H_5OH	Various
Oxygen content (% mass)	34.8	0
Density (kg/L)	0.79	0.74
Research Octane Number	109	95
Stoichiometric air-fuel ratio	9	14.7
LHV (MJ/kg)	26.95	42.9
Boiling point(°C)[5]	78.4	25-215
Latent heat (kJ/kg)[5]	904	380-500

Source [5] and [6]

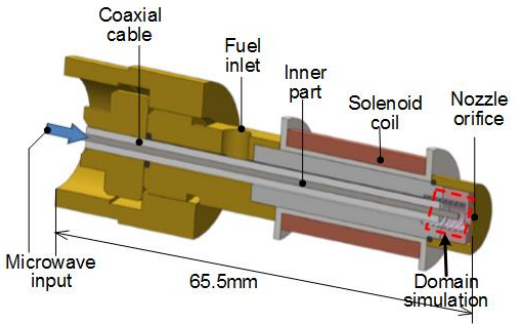

Fig. 1. Schematic view of LMI system.

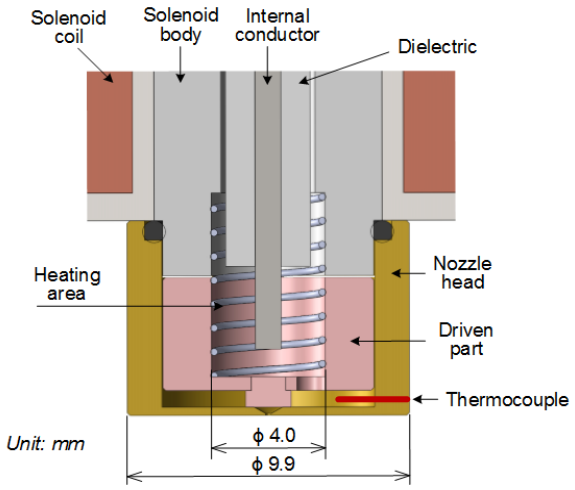

Fig. 2 Closed view of LMI injector head.

2 Methods

2.1. Numerical Simulation

Numerical simulation on 3D geometry of heating zone was performed in COMSOL Multiphysics to solve the electromagnetic, heat transfer and momentum transport equations. Electric field distribution in the heating zone is calculated based on the equations below [17-18]:

$$\nabla \times \frac{1}{\mu_r}(\nabla \times E) - k_0^2(\varepsilon_r - \frac{j\sigma}{\omega\varepsilon_0})E = 0 \qquad (1)$$

Where E is electric field (V/m), ε_0 is free space permittivity (8.854×10^{-12} F/m), ε_r is relative permittivity, μ_r is relative permeability, σ is electric conductivity (S/m), k_0 is wave vector number, and ω is angular wave frequency (rad/s).

Volumetric energy (Q) generated by microwave heating inside material can be calculated from the electric field intensity using equation below:

$$Q = \omega \varepsilon_0 \varepsilon^{"} |E|^2 \quad (2)$$

Energy balance equation of microwave energy heat can be used to calculate temperature distribution as follow:

$$\rho c_p \frac{\partial T}{\partial t} + \rho c_p u \cdot \nabla T = \nabla \cdot (k \nabla T) + Q \quad (3)$$

Where T is temperature (K), ρ is density(kg/m^3), $\varepsilon"$ is dielectric loss (F/m), c_p is specific heat (J/kgK), u is axial velocity (m/s) and k is thermal conductivity of material (W/mK).

Continuity and momentum equation of fluid flow are solved in transient forms as follows:

$$\rho \frac{\partial u}{\partial t} + \rho(\nabla \cdot u) = 0 \quad (4)$$

$$\rho \frac{\partial u}{\partial t} + \rho(u \cdot \nabla)u = -\nabla p + \mu \nabla^2 u + \rho g \quad (5)$$

Where p, μ, g are pressure (Pa), viscosity (Pa.s), and gravity (m/s^2) respectively.

Schematic of geometry and boundary condition of this study can be seen in Fig.3. Two models of the inner part, square and round model, were compared and each model varied in diameter of inner part material of 1.2mm, 1.6mm and 2.0mm respectively.

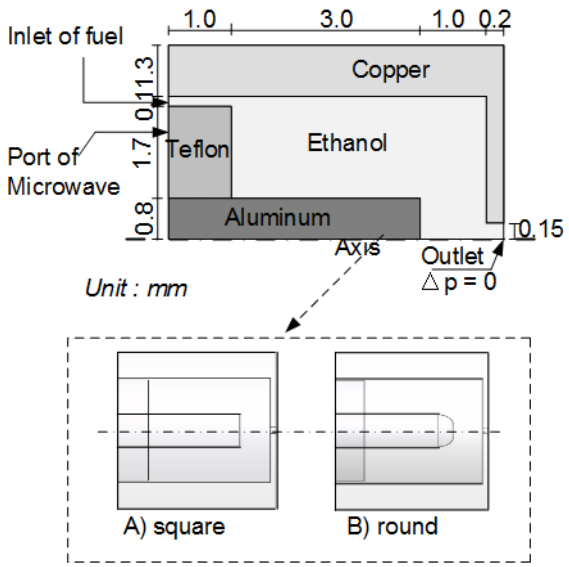

Fig. 3. Schematic geometry and two differences model of inner part.

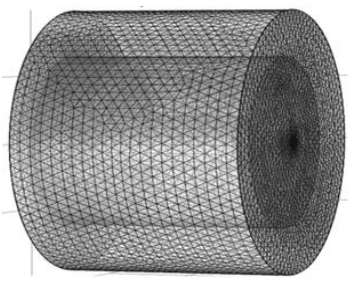

Fig. 4. Mesh stucture of simulation domain

2.1.1. Initial conditions.

At the initial process of this study, the temperature of the fuel is assumed in the thermal equilibrium with the surrounding temperature at 293K. Electric power imposing into the system was set to constant value of 60Watt.

2.1.2. Boundary conditions and mesh.

Wall materials of heating zone consist of metallic material, hence the electric field and magnetic field can be perfectly reflected from this conductor material. Boundary conditions on this wall can be expressed as below [18, 19]:

$$n \times E = 0 \text{ and } n \cdot H = 0 \quad (6)$$

Where n is normal to surface of the wall, E is electric field and H is magnetic field.

Ethanol is used as the working fluid with operating pressure of 0.3Mpa. Dielectric properties of the fuel used in this simulation consist of dielectric permittivity (real 24.3 and imaginary 22.86) and dielectric permeability of 1.67 as in [20]. Teflon, a dielectric material, is used as a guide passage of the electromagnetic wave from magnetron to the heating zone. This material has dielectric permittivity 2.1, dielectric permeability 1.0 and the electric conductivity of 1e-32S/m [21]. Free convection heat transfer with coefficient convection 5W/m/K to the ambient temperature of 293.15K was considered at the outside cover of injector wall. An electromagnetic wave equation was solved at constant frequency 2.45GHz and power input of 60Watt.

Geometry and boundary conditions used in this study can be seen in the next Fig.3. Heating area was developed in cylindrical shape with length of 4mm. The geometry was discretized into finite volume method and solved in the time dependent state. For more accurate simulation results, fine mesh structure was simply used for fluid phase and normal mesh structure used for solid phase that provided finer enough mesh for microwave heating. The fine mesh structure was used for fluid flow problem to resolve the thin boundary layer along the fluid boundary. Total mesh generated in the simulation domains was 133,874 element meshes (Fig. 4). COMSOL Multyphysiscs provides an automatic adapted mesh generation for solving complex algebraic equations applied to the system [22]. Spatial and temporal heating characteristic

inside the LMI system are the main focus of this analysis.

Nonlinear partial differential equations applied in this study were solved using an implicit method of Backward Differentiation Formula (BDF) solver. Multifrontal massively parallel sparse direct solver (MUMPS) scheme was applied for solving the transient solution of temperature and other phenomena related to this heating process.

2.2. Experimental measurement

A comprehensive measurement on temperature profile at tip injector and spray characteristic of fuel spray was performed to analyze the effect of microwave heating on spray formations. Layout of the experimental apparatus can be seen in Fig.5. Heating time was adjusted 20msec over 40msec operation cycle, whereas injection time was set 5ms over 200ms (Fig. 6). A power source of 60Watt was imposing into the microwave power during heating.

Temperature of fuel at tip injector was measured at the tip injector using K-type thermocouple whereas the spray characteristics of injected fuel were evaluated using backlight imaging and laser particle analyzer techniques. Droplet size in term of Sauter Mean Diameter (SMD) and particle distribution of the spray were investigated using Laser Diffraction Spray Analyzer (LDSA) whereas the spray components such as liquid shell, ligaments and droplets were evaluated using imaging system in high speed camera.

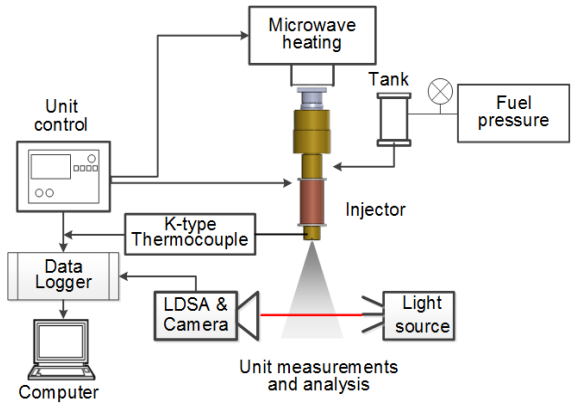

Fig. 5 Schematic of experimental apparatus

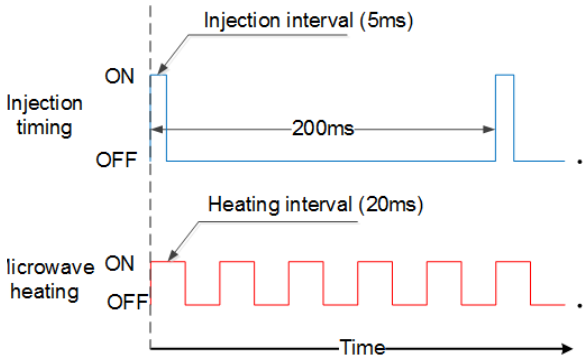

Fig. 6. Injection time and input signal controll for injection and heating process.

3 Results and Analysis

3.1. Electromagnetic heating

Fig. 7 shows the electric field distributions inside the heating zone of two model simulated. It shows that maximum electric field distribution is formed around the tip of the inner conductor. This characteristic can happen due to the combination of incident and reflection wave power from the wall as well as the penetration depth in the material. Polarization of electric power at high frequency is increasing the energy released into ethanol inside the heating zone [23]. The electric field attenuation tends to increase the energy absorption which increases the temperature of ethanol as described in [24]. The consequence of the electric field distribution can be seen in the increasing of temperature generated around the corner of the inner conductor.

Fig. 8 represents the dissipated energy generated by electromagnetic wave inside the heating zone. The contour distribution of power dissipated density in this system is proportional to the spatial and temporal of electric field distribution. It can be seen that power heating is concentrated at the corner of the tip conductor, reaching maximum values of 14.4e9W/m2 and 9.3e9W/m2 for square and round model respectively. Tthe total absorption of

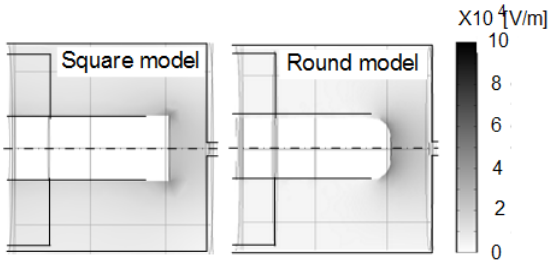

Fig. 7. Electric field distribution.

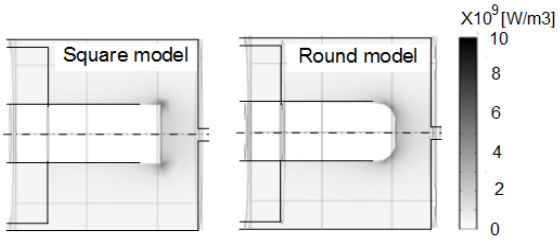

Fig. 8. Volumetric energy dissipation during imposing microwave into the system.

microwave power from adjacent surfaces of the wall forming in the edge corner of inner part is expected to the main contribution on this phenomena. The distribution characteristics of microwave power absorption in this model are similar as found in [25]. Distribution of power dissipated remains constant during imposing microwave into the system.

The distribution of electric field normalization inside heating area of three differences of inner diameter can be seen in Fig.10. It was evaluated at 0.2mm from the surface of all inner conductors along the heating zone. In the square model, the electric field is mainly generated at the edge of inner tip and it is increased by the decreasing of inner conductor diameter. A few differences in the square model in which the peak of electric fields became lower and moved a slight far from the tip of the inner conductor. Moreover the smaller the inner diameter of the inner part, the higher the impedance of coaxial cable that probably increases the electric field intensity inside material.

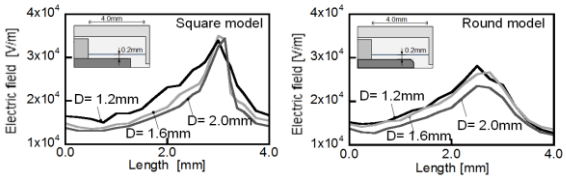

Fig. 10. Electric field distribution along the surface of inner part.

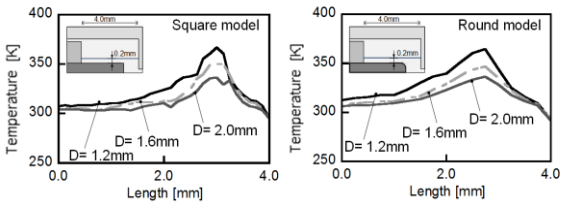

Fig. 11. Temperature distribution along the surface of inner part conductor.

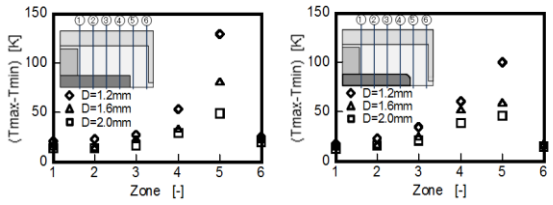

Fig. 12. Gradient temperature at 6 specific points along the heating zone.

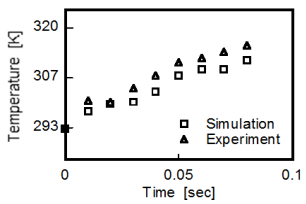

Fig. 13. Temperature of the fuel at injector tip.

Temperature field distributions generated in the different heating zone of two models compared can be seen in Fig.11. Rapid heating of ethanol is occurring short time after imposing electromagnetic power into the system. However, it is obviously that the uneven distribution of temperature is still dominant and hot spot appearances in the edge of the inner part. For square model, hot spot occurs in the corner or edge of the inner part, whereas for round model, temperature of the fuel becomes expanded along the tip surface of the inner part. This phenomenon can happen due to higher thermal absorption and flux distribution of the electromagnetic field at this area [26-27]. The electric field is concentrated in this place due to the standing wave of electric field from the metal walls surrounded the fuel. The oscillation of incident and reflection wave power from the wall creates the net of electric field intensity in this region causing the concentration and produces hotspot at this corner. The maximum temperature field in the square model is 367K, 350K and 340K for inner diameter 1.6mm, 1.8mm and 2.0mm, respectively. In round model the maximum temperature is 365K, 347K and 337K for inner conductor diameter 1.6mm, 1.8mm and 2.0mm, respectively.

Fig.12 shows the trend of temperature gradient generated in the sixth (6) differences zone along heating area. In square model the maximum gradient temperature derives at zone 5 around the tip of the inner part, with gradient temperature maximum of 49.2K, 81.5K, and 129.2K for inner part diameter of 1.2mm. 1.6mm and 2.0mm respectively. For round model, the maximum gradient temperature are 46.5K, 59.5K, and 100.2K for inner part diameter of 1.2mm. 1.6mm and 2.0mm, respectively. The strength of electromagnetic field inside heating zone affects the heating characteristics of the model simulated. The small changing in the size and geometry of heating zone influences accordingly on the electromagnetic wave distribution and leads to the various result of energy dissipation

Fig. 13 shows the comparison result between experiment and simulation of the fuel temperature at tip injector during heating. It shows that the trend of temperature distribution in the simulation result agrees fairly well with experimental measurement. Temperature of injected fuel increased rapidly during imposing electromagnetic energy into the

system. In 100msec time heating the temperature of fuel injected measured at tip injector increased around 22°C. The slight difference in some points, however, is due to the sensitivity of electric field in the zone as well as the simplified model simulation from the complex geometry of LMI system.

3.2. Fuel spray characteristics

Spray performances of the LMI system were experimentally evaluated using LDSA and high speed camera. Droplet diameter of fuel spray can be evaluated directly using LDSA device whereas spray formation can be seen in the recording camera (PHOTORON FASTCAM SA5). In order to understand the spray formation, the images captured were analyzed using image processing software (Images-J and Memrecam HXLink).

Fig.14 shows the droplet size in term of SMD (Sauter Mean Diameter) and the droplet distributions between heating and non-heating spray. It is the evidence that microwave heating affects the properties of fuel, and consequently the droplet size can be reduced when the ethanol exposed microwave energy heating. In this experiment, it can be seen also that droplet size of heating spray decreases significantly (around 50%) from the average diameter of 80µm in non-heating spray.

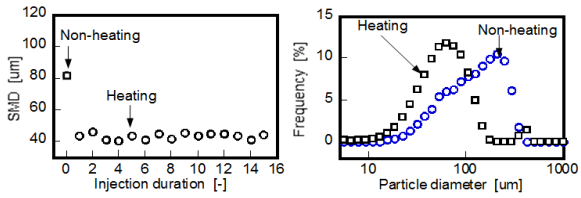

Fig. 14. SMD and droplet size distribution between heating and non-heating spray.

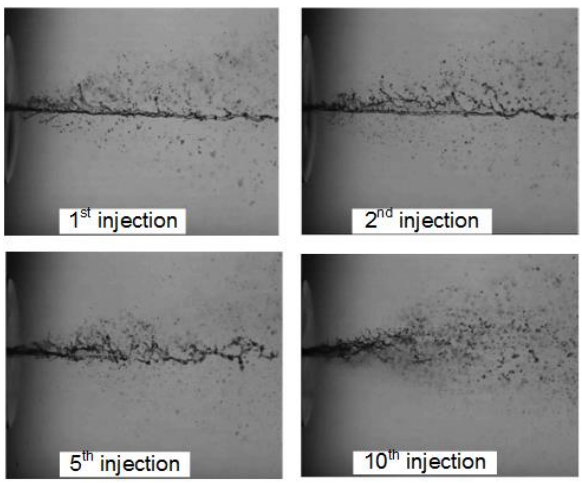

Fig. 15. Volumetric energy dissipation during imposing microwave into the system

The smaller diameter observed in heating fuel may arise from the reducing in fuel density, viscosity and surface tension due to increasing temperature. Fig. 15 shows the spray component distributions of ethanol at several time injections. It is clear that in the early injection the liquid films are dominant in the spray image and gradually changed into a small droplets size during increasing the temperature of the fuel. The amount of small droplets is large in the next injection as the temperature rises. An increasing in fuel temperature reduces the viscosity and surface tension of ethanol and makes easy breakup the droplet spray. This could offer an interesting application for atomization of ethanol and other bio-component fuel in such injector applications.

Image analysis was also performed to understand the microwave heating effect on droplet atomization. Several images captured during injection were processed in image-J and Memrecam software. The background noise of the images can be eliminated by subtracting the images and later thresholded to extract the droplet size. Subtracted background also makes the distance of background pixel become plate, thus, it can easily perform the binarization of spray photos. Adjusting the threshold number is critical for the droplet size analysis since it is related to the spatial area and the diameter of droplets in the spray.

Fig. 16 explores the droplets distribution of heating and non heating spray based on the images analysis. The number of droplets in the heating fuel is bigger than that in the non heating fuel. SMD provided in heating fuel can reach 624um while in non-heating fuel can reach around 895um.

Figure 17. and Fig. 18 show a series of puffing spray photos extracted from the specific location of the spray. This analysis is proposed to evaluate the liquid component in the spray dispersed into smaller droplets between heating and non heating fuel. Thresholded images spray provide clear information of spray formation and dispersion after heating. In the heated spray, the liquid spray changes into the finer droplet in the short time which means the

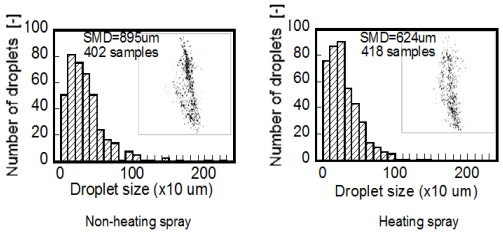

Fig. 16. Images analysis of droplets size on heating and non -heating spray fuel.

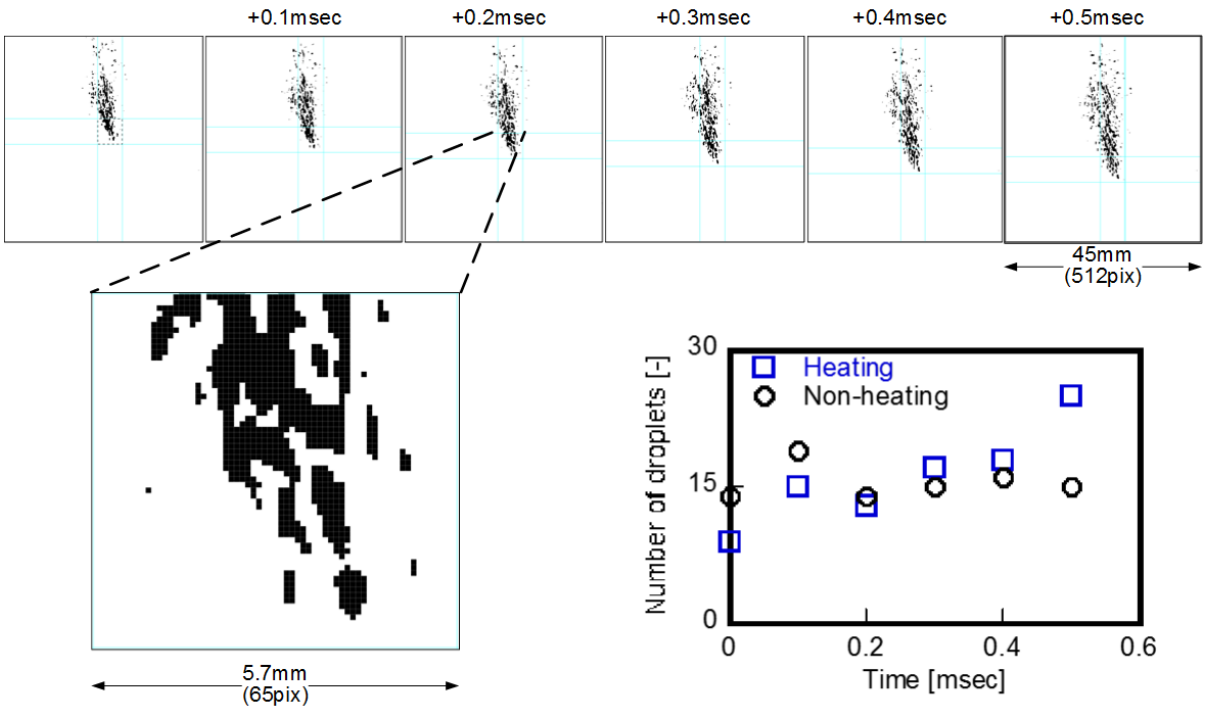

Fig. 17 Characteristic of sprayed droplets during increasing the time of injection.

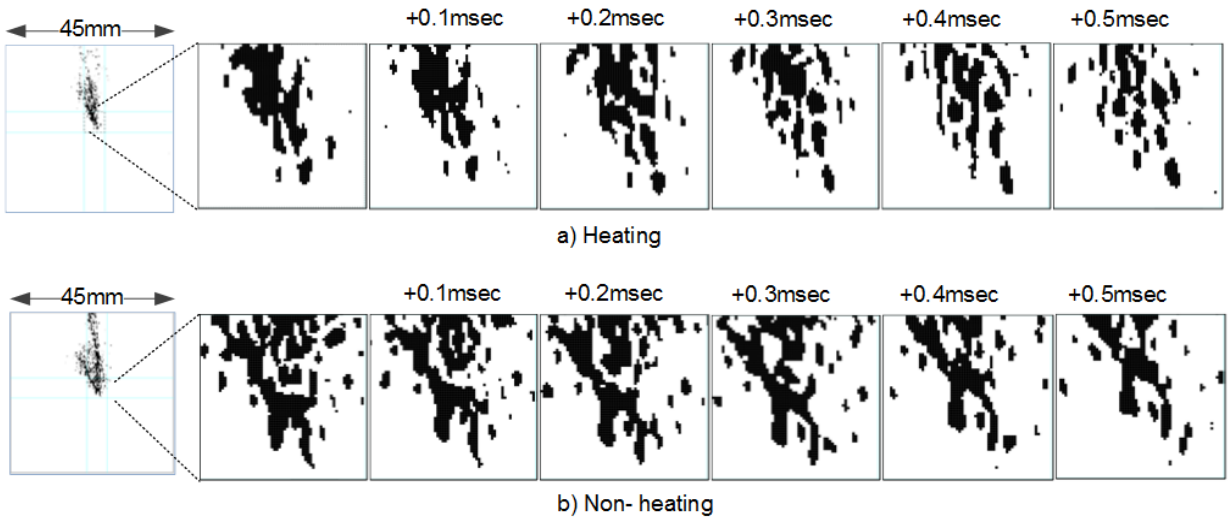

Fig. 18 Two different views of droplet structure for heating and non-heating fuel.

surface volume area became dispersed in to several parts. The liquid fuel of heated spray at the specific location was completely changed into small droplets component in around 0.5msec after experienced microwave heating (Fig, 17). During the time of 0.5 msec the number of droplets in the heating spray become higher than in the non-heating spray. It clearly shows the fundamental effect of microwave heating on the spray breakup model of fuel injected.

4 Conclusion

A comprehensive studies have been performed to investigate the microwave heating process of ethanol as well as the spray characteristics of the fuel injected from the LMI system. The conclusions can be summarized as following:

(1). The geometry of the heating zone is important in the heating performance of the LMI system. Energy absorption was found to increase when

the inner part diameter is smaller, where the electric field density becomes increasing. This phenomena affect the temperature field distribution in the heating zone. Slight changes in the inner part tip affect also on the distribution of hot spot temperature in the ethanol.

(2). The electric field intensity of the heating zone varies considerably with inner part diameter. Electric field distribution tends to increase by reducing the inner diameter, which affect the large amount of fluid volume inside the zone, and leads to rise the electromagnetic wave oscillation and to increase the temperature of the fuel.

(3). Experimental and imaging analysis shows the critical of microwave heating on the spray formation of fuel. Droplets of fuel were dispersed into several small droplets shortly after imposing elelctromagnetic power in the LMI system. An improvement on spray characteristics of fuel heated is expected to enhance fuel atomization and evaporation for high performances combustion.

Advance experiment and simulation studies are important for the fuel stream inside the engine as well as the engine performances and emissions characteristics during microwave heating from LMI system. Further study is also needed for higher injection pressure of the fuel.

Aknouledgement

This work was supported by the collaboration of Higher Education Department of Republic Indonesia and Kanazawa University Japan.

References:

[1] Costa RC, Sodre JR, Compression Ratio Effect on Ethanol/Gasoline Fuelled Engine Performance, Applied Thermal Engineering, Vol. 31, 2011; pp.278-283

[2] Aleiferis, P.G., Pereira, J.S., van Romunde, Z., Caine, J., Wirth, M., Mechanisms of spray formation and combustion from a multi-hole injector with E-85 and Gasoline, Combustion and Flame, Vol. 157, 2010, pp.735-756.

[3] Padala S, Le MK, Kook S, Hawkes ER, Imaging diagnostics of ethanol port fuel injection sprays for automobile engine applications, Applied Thermal Engineering, Vol. 52, 2013; pp.24-37.

[4] Park SH, Kim HJ, Suh HK , Lee CS, Atomization and spray characteristics of Bioethanol and Bioethanol Blended Gasoline Fuel Injected Through a Direct Injection Gasoline Injector, Int. J. of Heat and Fluid Flow, Vol. 30, 2009, pp.1183-1192.

[5] Matsumoto A, Moore WR, Lai M, Sheng Y, Foster M, Xie X, Yen D, Confer K, Hopkins E, Spray Characterization of Ethanol Gasoline Blends and Comparison to a CFD Model for a Gasoline Direct Injector, SAE Paper 2010-01-0601, 2010.

[6] Vancoillie J, Demuynck J, Sileghen L, Van De Ginste M, Verhelst S, Brabant L, Van Hoorebeke L, The potential of methanol as a fuel for flex-fuel and dedicated spark-ignition engines, Applied Energy, Vol. 102, 2013, pp.140-149.

[7] Gumus M, Reducing cold-start emission from internal combustion engine by means of thermal energy storage system, Applied Thermal Engineering,Vol.29, 2009, pp.652-660.

[8] Kabasin D, Hoyer K, Kazour J, Lamers R, Hurter T., Heated injector for ethanol cold starts, SAE International 2009-01-0615; 2009.

[9] Sales LCM, Sodre JR, Cold start characteristics of an ethanol-fuelled engine with heated intake air and fuel, Applied Thermal Engineering, Vol.40, 2012, pp.198-201.

[10] Enomoto H, Nozue H, Hieda N, Validation of heatup effect on ethanol spray with local-contact microwave-heating injector by using image analysis, Transaction of JSME, Vol. 80, No. 820, 2014, P. TEP036 (In Japanese).

[11] Tran THT, Enomoto H, Nishioka K, Kushita M, Sakitsu T, Ebisawa N, Effect of ethanol ratio and temperature on gasoline atomizing using local-contact microwave-heating Injector, SAE Paper 2011-32-0582; 2011.

[12] Mangalla LK, Enomoto H, Nozue H. Teraoke Y., Hieda N., Numerical Simulation of Heating Zone Detailed Structure in the Local-contact Microwave-heating Injector, Proceeding of Grand Renewable Energy in Tokyo 2014, Part O-Bm-7-4.

[13] Sharma G, Prasad S, Specific energy consumption in microwave drying of garlic cloves, Energy Vol. 31, 2006, pp. 1921-1926.

[14] Yoshikawa N, Fundamentals and applications of microwave heating of metals, Journal of Microwave Power and Electromagnetic Energy Vol. 44, No.1, 2010, pp.4-13.

[15] Mangalla LK, Enomoto H, Spray characteristics of Local-contact Microwave-heating Injector Fuelled with Ethanol, SAE Paper 2013-32-9126; 2013.

[16] Kotek L., Pistek P., Jonak M., Bivariate Process Capability Analysis of Fuel Injection Nozzles Production, WSEAS Transaction on Heat and Mass Transfer, Vol. 10, 2014, pp.491-495.

[17] Salvi D, Boldor D, Aita GM, Sabliov CM, Comsol multiphysics model for continuous flow microwave heating of liquid, Journal of Food Engineering Vol. 104, No. 3, 2011, pp. 422-429.

[18] Cuccurullo G., Giordano L., Viccione G., Quantitative IR Thermography for Continous Flow Microwave Heating, WSEAS Transaction on Heat and Mass Transfer, Vol. 9, 2014, pp.234-242.

[19] Knoerzer K, Regier M, Scubert H, A computational model for calculating temperature distribution in microwave food application, Innovative Food Science and Engineering Technologies, Vol. 9, 2008, pp 374-384.

[20] Wyman J, Dielectric constants of ethanol- ether and urea-water, Journal of the American Chemical Society, Vol. 55, No. 10, 1933, pp. 4116-4121.

[21] Xiang, F., Wang, H., and Yao, X., Preparation and Dielectric Properties of Bismuth-Based Dielectric/PTFE Microwave Composites, Journal of the European Society, 26:10-11, 2006, pp. 1999-2002.

[22] Campo A., Celentano D.J.,Robbins J.E., Fast Numerical Calculation of Conduction Shape Factors with the Finite Element Methods in the COMSOL Platform, WSEAS Transaction on Heat and Mass Transfer, Issue. 4, Vol. 7, 2012, pp.91-104.

[23] Zhu J, Kuznetsov AV, Sandeep KP, Mathematical modeling of continuous flow microwave heating of liquids (effect of dielectric properties and design parameters), International Journal of Thermal Science , Vol. 46, 2007, pp. 328-341.

[24] Tada S, Echigo R, Yoshida H, Numerical analysis of electromagnetic wave in a partially loaded microwave applicator, Int. Journal of Heat Mass Transfer, Vol. 41, No.4-5, 1998, pp.709-718.

[25] Acevedo L, Uson S, Uche J, Exergy transfer analysis of microwave heating system, Energy Vol. 68, 2014, pp. 349-63.

[26] Hossan MR,. Byun DY, Dutta P, Analysis of microwave heating for cylindrical shape object, Int. Journal of Heat and Mass Transfer, Vol. 53, 2010, pp. 5129-5138.

[27] Chandrasekaran S, Ramanathan S, Basak T, Microwave food processing – a review, Food Research International, Vol. 52, 2013, pp. 243-261.